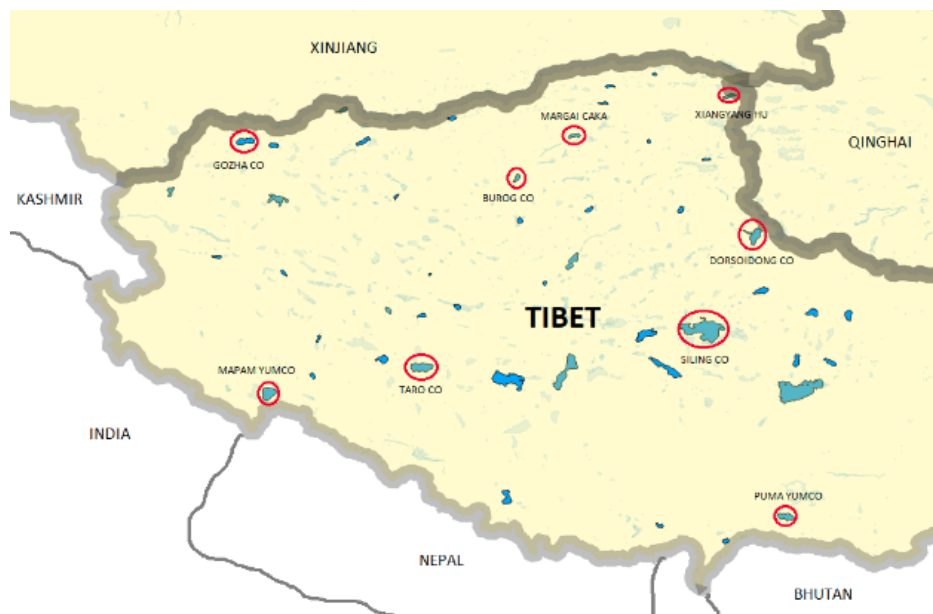


# Water Level Analysis in Tibet using CryoSat-2

*-Revised version-*



Bachelorarbeit im Studiengang  
**Geodäsie und Geoinformatik**  
an der Universität Stuttgart

Lun Yan

Stuttgart, Januar 2019

**Betreuer:** Dr. Hassan Hashemi Farahani  
Universität Stuttgart

Prof. Dr.-Ing. Nico Sneeuw  
Universität Stuttgart



# Erklärung der Urheberschaft

Ich erkläre hiermit an Eides statt, dass ich die vorliegende Arbeit ohne Hilfe Dritter und ohne Benutzung anderer als der angegebenen Hilfsmittel angefertigt habe; die aus fremden Quellen direkt oder indirekt übernommenen Gedanken sind als solche kenntlich gemacht. Die Arbeit wurde bisher in gleicher oder ähnlicher Form in keiner anderen Prüfungsbehörde vorgelegt und auch noch nicht veröffentlicht.

Ort, Datum

Unterschrift



# Abstract

While the water level monitoring in Tibet suffers data gaps due to insufficient in situ gauge stations, the satellite altimetry serves as an efficient alternative. In this work, measurements from the CryoSat-2 mission are employed and analyzed to determine water level time series in various lakes throughout Tibetan region. The time series are calculated by reducing the geoid undulations from surface heights measured and provided in CryoSat-2 level-2 products. They are also subjected to a novel outlier detection scheme to identify and eliminate outliers. Combined with the local geography, the water level time series can deliver an overview of hydrological pattern throughout Tibet.



# Contents

<b>1</b>	<b>Introduction</b>	<b>1</b>
1.1	Background . . . . .	1
1.2	Study area . . . . .	2
1.3	CryoSat-2 . . . . .	3
<b>2</b>	<b>Methodology</b>	<b>5</b>
2.1	Water level determination . . . . .	5
2.2	Choice of the geoid . . . . .	7
2.3	Outlier detection scheme . . . . .	10
2.3.1	Step 1: global . . . . .	13
2.3.2	Step 2: track-wise . . . . .	13
2.4	Trend computation . . . . .	14
<b>3</b>	<b>Result</b>	<b>15</b>
3.1	Selected lakes . . . . .	16
3.1.1	Geographic illustrations . . . . .	16
3.1.2	Water level time series . . . . .	18
3.2	Hydrological pattern . . . . .	20
<b>4</b>	<b>Conclusion</b>	<b>23</b>





## List of Figures

1.1	Tibetan lakes . . . . .	2
1.2	CryoSat-2 mode mask provided by ESA ( <a href="https://earth.esa.int/web/guest/-/geographical-mode-mask-7107">https://earth.esa.int/web/guest/-/geographical-mode-mask-7107</a> ) . . . . .	3
2.1	Calculation of water level . . . . .	6
2.2	Geoid difference in Tibet (Eigen6C4 minus EGM2008) . . . . .	8
2.3	Geoid difference in Tibet zoomed (Eigen6C4 minus EGM2008) . . . . .	8
2.4	Measurements before outlier detection . . . . .	11
2.5	Measurements after outlier detection step 1 . . . . .	11
2.6	Measurements after outlier detection step 2 . . . . .	11
2.7	Histogram of the time series before outlier detection . . . . .	12
2.8	Histogram of the time series after outlier detection step 1 . . . . .	12
2.9	Histogram of the time series after outlier detection step 2 . . . . .	12
2.10	Time series . . . . .	14
3.1	Dorsoidong Co . . . . .	16
3.2	Mapam Yumco . . . . .	16
3.3	Xiangyang Hu . . . . .	16
3.4	Margai Caka . . . . .	16
3.5	Siling Co . . . . .	17
3.6	Burog Co . . . . .	17
3.7	Gozha Co . . . . .	17
3.8	Puma Yumco . . . . .	17
3.9	Dorsoidong Co . . . . .	18
3.10	Mapam Yumco . . . . .	18
3.11	Xiangyang Hu . . . . .	18
3.12	Margai Caka . . . . .	18
3.13	Siling Co . . . . .	19
3.14	Burog Co . . . . .	19
3.15	Gozha Co . . . . .	19
3.16	Puma Yumco . . . . .	19
3.17	The water level trends of lakes in Tibet . . . . .	20



# Chapter 1

## Introduction

This chapter introduces the background of water level analysis, the study area as well as the satellite mission CryoSat-2. Chapter 2 deals with its methodology along with the example of Taro Co (a lake in southwest of Tibet). Chapter 3 shows the result of a few selected Tibetan lakes using the same methodology. And in the last chapter, a conclusion is drawn.

### 1.1 Background

Climate change is a great concern of the 21 century. It is a problem at international, regional, national and local levels. Events related to uncertain climatic conditions such as floods, droughts, landslides, high waves, and sea level rise are increasingly common with increasing intensity, resulting in casualties in economic and ecological losses (IPCC, 2018 [1]). Scientists worldwide have been using theoretical models and observations to understand its past and future. Lake systems are essential to be monitored and analyzed, as they continually respond to climatic conditions that vary over broad scales of space and time.

The spatial distribution of lakes on the Earth's surface indicates long-term patterns of atmospheric circulation, and the lake hydrological and energy balances are coupled to the atmosphere. In response to the inputs of mass, energy, and momentum (precipitation, radiation, and wind stress), lakes return heat and moisture to the atmosphere through conduction and evaporation. Global, regional, or local changes in the hydrological or thermal states of lakes thus represent interactive responses to climatic variation in the supply of water and energy (Hostetler, 1995 [5]). It is believed that the water level of the lakes is crucial to be monitored. However, the number of global in situ measurements of gauges has been declining since the 1980s. Substantial delays in data access and large declines in monitoring capacity prevent an accurate analysis of the recent past (Vörösmarty et al., 1999, 2000c [11]). Especially in Asia, almost no in situ data are available. This gives rise to data gaps in water level measurements of the lakes. In fact, there are only few in situ stations in the areas where not many people are living. Those areas, however, usually have large amount of natural resources, especially water. Thus, new techniques are required to realize water level monitoring there.

One such technique is satellite altimetry. Since a satellite has a giant coverage on Earth, it may allow unprecedented accuracy in the quantification of the global hydrological cycle. In the recent years, there are a few satellite altimetric missions including TOPEX/Poseidon, ERS, ENVISAT and Jason. But none of them was designed primarily for monitoring inland waters. Another satellite mission named CryoSat-2 is very useful, though. In fact, it is strongly related to the study area of this work.

## 1.2 Study area

Known as *the third pole* on the Earth, Tibet is a very interesting area for both scientific analysis and economic development (see Fig. 1.1). The Tibetan plateau especially has an average elevation of over 4500 m and an area of around 2 500 000 km<sup>2</sup>. There are approximately 400 lakes in the Tibet, over half of them larger than 10 km<sup>2</sup>. These lakes are, along with climate change and global warming, very essential natural resources. The studies of the integrated, global nature of the hydrological cycle are essential to our understanding of natural climate variability and to predict a climatic response to anthropogenic forcing. (Koster et al., 1999 [8]) The water levels of the lakes are thus to be monitored and analyzed.

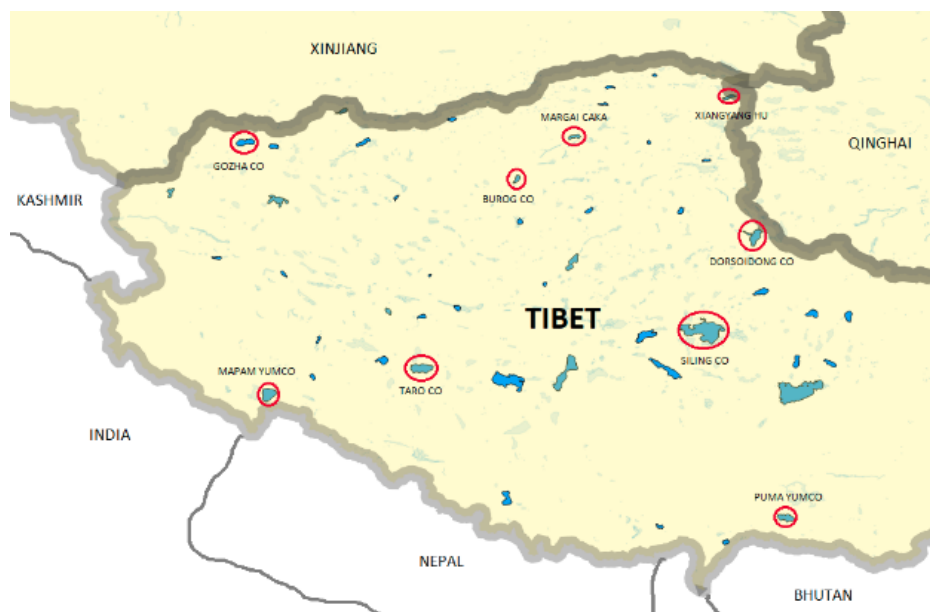


*Figure 1.1: Tibetan lakes*

Due to low population in a large area as mentioned before, Tibet suffers insufficient number of in situ gauge measurements of the water levels. Especially small lakes are not monitored properly. Even for large lakes, the in situ measurements are not covering them completely. When taking the temporal effect into consideration, the water level measurements have big gaps in the data, which makes the monitoring and analysis rather difficult. New techniques are therefore required to deal with data gaps. There have been many studies over Tibetan area, e.g., the work by Delft University of Technology (Kleinherenbrink et al., 2014 [6]). That work presented the application of CryoSat SARIn mode data to monitor lakes in mountainous areas. But it didn't manage to deliver a hydrological pattern of water levels. In this work, nine lakes in Tibet are selected. Their names are Taro Co, Dorsoidong Co, Mapam Yumco, Xiangyang Hu, Margai Caka, Siling Co, Burog Co, Gozha Co and Puma Yumco. They are well distributed in Tibet (see Fig. 1.1) and are in adequate size. The altimetry data are also available. For each lake, a 2D geographic figure with ground tracks as well as a time series figure including trend are generated. Finally, an overview of hydrological pattern of water levels throughout Tibet is shown and that is the main finding of this thesis. The results can be found in chapter 3.

## 1.3 CryoSat-2

One such technique to deal with data gaps involves the use of data collected by satellite altimetry mission CryoSat-2. CryoSat-2 is an European Space Agency (ESA) environmental research satellite. Launched in April 2010, CryoSat-2 is the first satellite carrying a delay-Doppler altimeter that operates in three measuring modes: Synthetic Aperture Radar (SAR) (green) is operated over sea-ice areas, some ocean basins and coastal zones. SAR Interferometric (SARIn) (purple) mode is used over steeply sloping ice-sheet margins, some geostrophic ocean currents, small ice caps and areas of mountain glaciers. Low Resolution Mode (LRM) (red) is operated over areas of the continental ice sheets, oceans and land not covered by other modes. For Tibet, as can be seen in Fig. 1.2, SARIn is responsible for its lakes. The two antennas used in the SARIn mode have an effect that the signal's main reflectance location can be determined. (Schneider, 2017 [10]) This gives an estimate of the exact location of the measurement, instead of the assumption that the measurement is placed directly at the nadir as with conventional SAR and LRM altimetry data. This mode also has the advantage of discriminating coastal echoes between land and water.

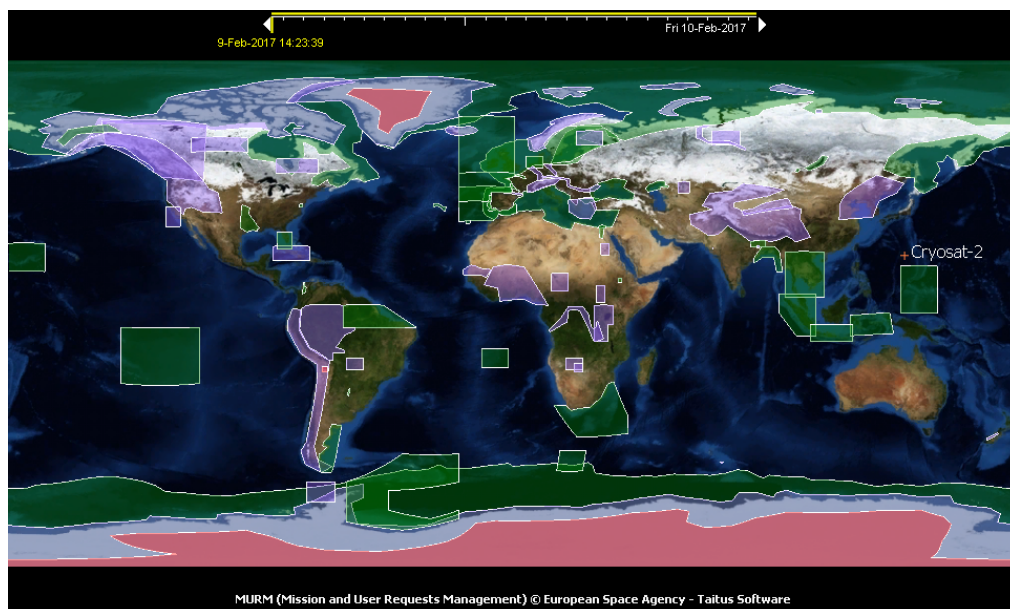


Figure 1.2: CryoSat-2 mode mask provided by ESA (<https://earth.esa.int/web/guest/-/geographical-mode-mask-7107>)

CryoSat-2 data can be downloaded from ESA's ftp server online (<ftp://science-pds.cryosat.esa.int>). To download the data, a username and password are available at the Institute of Geodesy at the University of Stuttgart. To read CryoSat-2 data in water areas, a python code was programmed. CryoSat-2 is able to acquire altimetric data continuously. It delivers a set of parameters, including the water level values and various corrections. The already processed L2 data from 2010 to 2018 serve as the input data for this work.



## Chapter 2

# Methodology

This chapter explains the methodology of the water level analysis using CryoSat-2. It is divided into four parts, i.e., calculation of water level, choice of the geoid, outlier detection scheme and trend computation. A lake named Taro Co (*Co* means *lake* in Tibetan) is used as an example to present the methodology. Its large size and good shape make it a good example to be analyzed. For the other selected lakes, the same methodology is then applied. Taro Co is located in southwest of Tibet, about 70 km<sup>2</sup> west of Coqên Town. It is a freshwater lake with an area of 486.6 km<sup>2</sup>. The average water level of Taro Co is approximately 4566 m. The lake area has a semi-arid climate with high and cold grassland.

### 2.1 Water level determination

First of all, the satellite data should be read and sorted. Then the data over the lake should be found, literally the crossing of the lake and the satellite groundtrack. This can be done by comparing the latitude and longitude of where the measurements are taken and the locations of the shapefiles of the lake. Tibetan lakes are located in the west of China, whose ESPG number is 4214 (important for the code).

The water level is actually the orthometric height of the water surface of the lakes. The following Fig. 2.1 illustrates the spatial relationship of the measuring distances and the orthometric height in question. The calculation is straightforward as:

$$h = A - R \quad (2.1)$$

and

$$H = h - N \quad (2.2)$$

with  $H$  being the orthometric height,  $h$  the ellipsoidal height,  $N$  the geoid undulation,  $A$  the altitude and  $R$  the range (with retracking correction).

The water levels are assigned to every 3D position. At the edge of the lake, a buffer zone of 0.15° (approximately 16.65 km) is created. The measurements in the buffer zone are eliminated in the first place due to the fact that the lake may shrink and expand. As mentioned before, the SARin mode has the advantage of discriminating coastal echoes between land and water. However, if the lake shrinks during the year, there is no longer water at the former edge of the

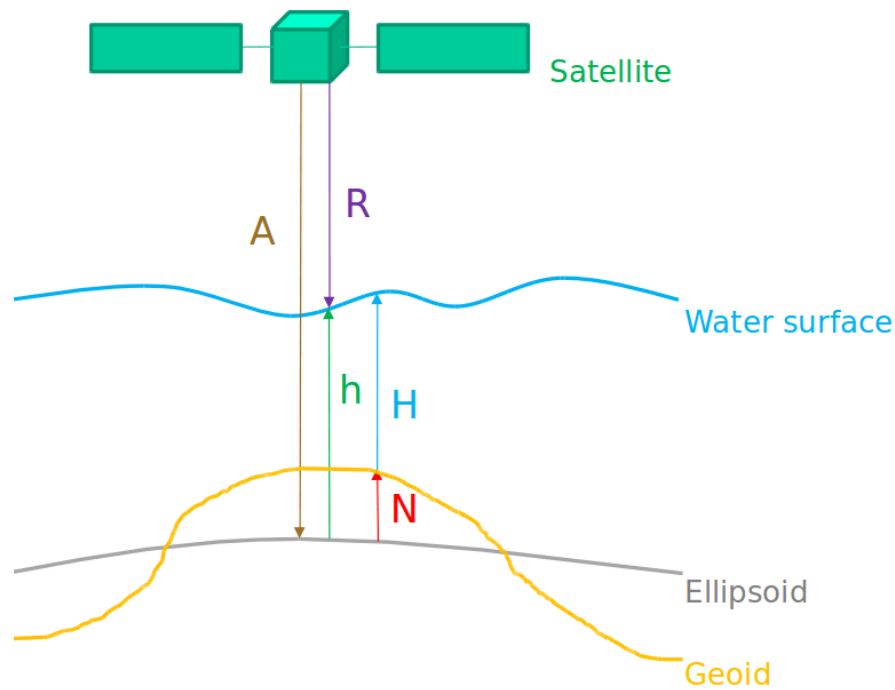


*Figure 2.1: Calculation of water level*

lake, which makes the satellite deliver wrong measurements. This is a source of the outliers. Note also that all of the measurements are not taken at the same time, but during the last eight years (2010-2018). So the variation of a few metres of the water level may be true if the lake rises or sinks in this long period.

In the programming process, each lake is chosen individually and the process takes much time. Due to huge amount of data read from ESA, it is a smart way to use a Python module named *pickle*, which enables objects to be serialized to files on disk and deserialized back into the program at runtime. It creates a PKL file from the CryoSat-2 data as the new input for the future in order to save time.



## 2.2 Choice of the geoid

As can be seen in the Eq. (2.2), the geoid undulation  $N$  plays a role in the determination of water level. Before this work, it has been a habit to use the geoid model EGM2008. EGM2008 vertical deflections over USA and Australia are within  $1.1'' - 1.3''$  of independent astrogeodetic values, which indicate great performance of EGM2008 with contemporary detailed regional geoid models (Pavlis, 2012 [9]).

For a long time, no specific doubts have been dropped on the choice of EGM2008. However, in this work, strange errors occur when using this geoid model. Although the EGM2008 fits North America, Europe and Australia well, it seems not suitable for Tibet due to its special location and geography. It is because EGM2008, designed by the National Geospatial-Intelligence Agency (NGA) of the United States uses a wealth of data in North America, Europe and Australia. But for Asia, South America and Africa, it may not fit well. Thus, it is crucial to choose a suitable geoid model which fits Tibet.

A well-fit geoid for Tibet area is generated by using online calculation service provided by International Centre for Global Earth Models (ICGEM, [icgem.gfz-potsdam.de/calc](http://icgem.gfz-potsdam.de/calc)), which delivers gravity field functionals on ellipsoidal grids. It uses the latest combined global gravity field model Eigen6C4 (Förste et al., 2014 [3]) of GeoForschungsZentrum (GFZ) Potsdam and Groupe Recherches Geodesie Spatiale (GRGS) Toulouse (Kostelecký et al., 2015 [7]). Eigen6C4 has been generated including the satellite gravity gradiometry data of the entire GOCE (Gravity and Ocean Circulation Experiment mission, see Floberghagen et al., 2011 [2]). For this work, the grid step is set to  $0.05^\circ$ . Using this geoid model, a matrix representing the geoid undulation is calculated. It is more current and has better accuracy. The difference of this matrix with the one from EGM2008 model for Tibetan area is illustrated in Fig. 2.2 and Fig. 2.3.

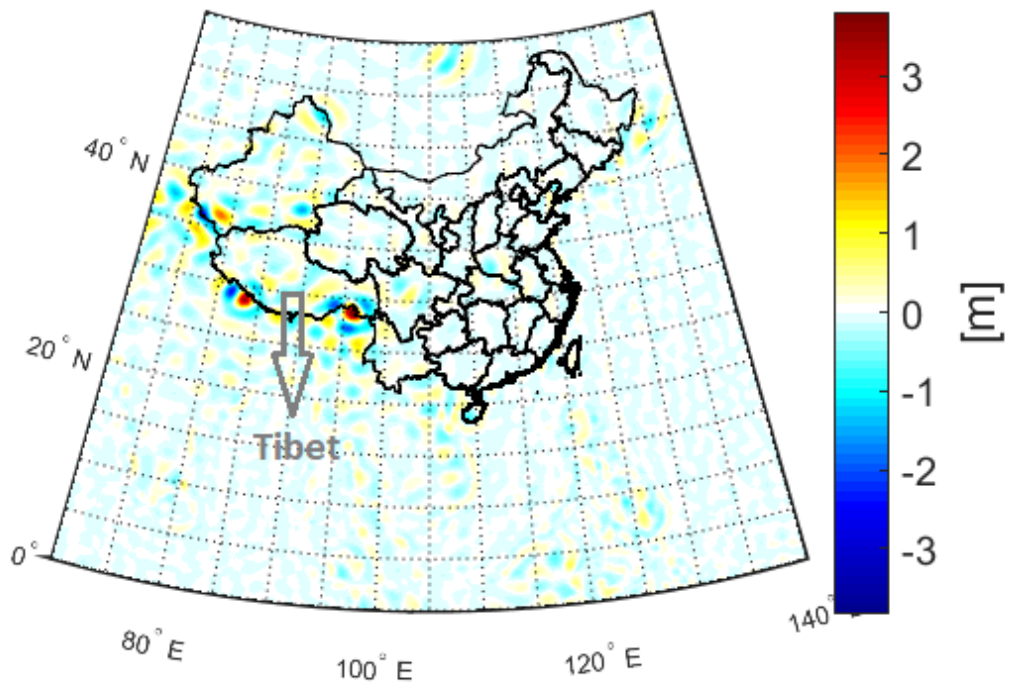


Figure 2.2: Geoid difference in Tibet (Eigen6C4 minus EGM2008)

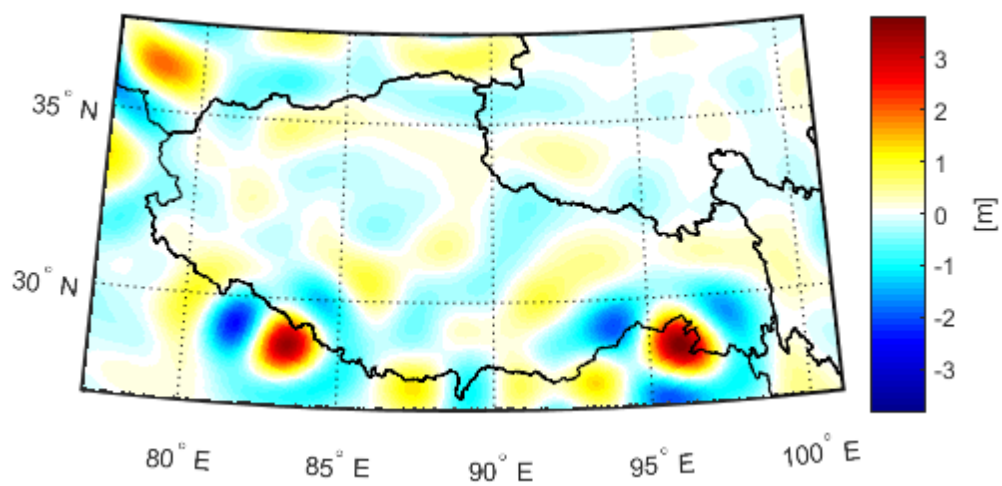


Figure 2.3: Geoid difference in Tibet zoomed (Eigen6C4 minus EGM2008)

The geoid difference ranges from around  $-3$  to  $+3$  metres globally, and this has to be taken into consideration. The white areas are those where the geoid matrix difference is zero or negligible. The areas in light blue or in light yellow have a difference of approximately 1 m. The interesting thing is that there are orange, dark blue and even red areas. They appear quite often near the Tibetan area especially. This also strengthens the importance of choosing a correct geoid model. Note that the administrative areas of China are shown in this figure in order to point out where Tibet is. The black lines and grey arrows and texts do not play any role for the values.

As this work was presented at INTERGEO 2018 in Frankfurt am Main, the geoid difference astonished the audience. One expert even doubted that the difference should be so big. In fact, the difference is almost null for North America, Europe and Australia. But it is really so big for many areas in Asia, South America and Africa, especially where there are huge mountains. When it zooms to Tibet (see Fig. 2.3), it can be seen that this area is close to the two red peaks, which means it is strongly affected by the geoid difference. As a result, the Eigen6C4 geoid model is chosen for the calculation of water level in Tibet, because it is more current.

## 2.3 Outlier detection scheme

Outlier detection has been used for centuries to detect and remove anomalous observations from data. Outliers arise due to mechanical faults, changes in system behaviour, fraudulent behaviour, human error, instrument error or simply through natural deviations in populations. (Hodge, 2004 [4]) As for the measurements in this work, an outlier detection is necessary. For one thing, the water level measurements carried out and delivered by the CryoSat-2 satellite are not perfect due to many effects on the satellite in space. Furthermore, the lakes on Earth are very related to water input, precipitation and water usage etc., which changes the condition of the lakes continuously. That is to say, both the tool to measure and the object to be measured may give rise to outliers in the measurements.

In order to detect the outliers in the measurements, an innovative way is used in this work. Since each measurement is associated with a global coordinate on Earth, i.e., a unique location, the water level is thus assigned to their locations. So it is practical to illustrate them with the geography of the corresponding lakes. As mentioned before, there is a buffer zone of 1.5 degrees (approximately 16.65 km) at the edge of the lake. This value is yet different for each lake. For bigger lakes, a bigger buffer may be used and vice versa. Inside the lake area, the ground tracks, where measurements are taken, should be seen clearly. There are obviously outliers in the water level values. The stepwise outlier detection is helpful for retrieving the good measurements from all. An overview of the four geographic illustrations, the corresponding histograms as well as the comparison and detailed analysis are as follows.

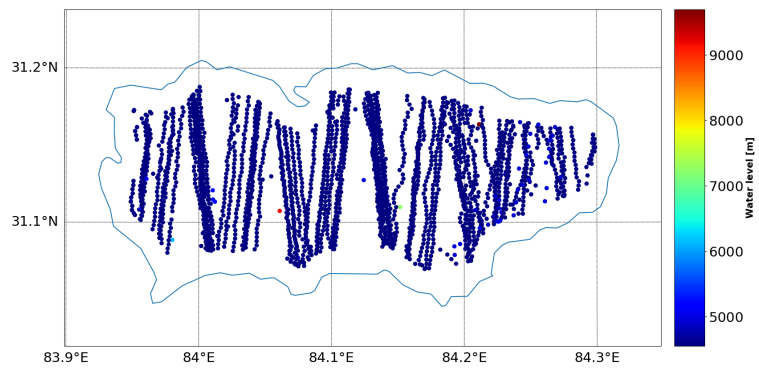


Figure 2.4: Measurements before outlier detection

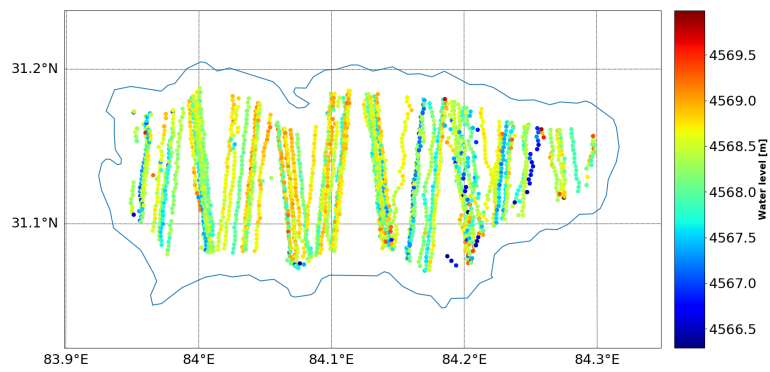


Figure 2.5: Measurements after outlier detection step 1

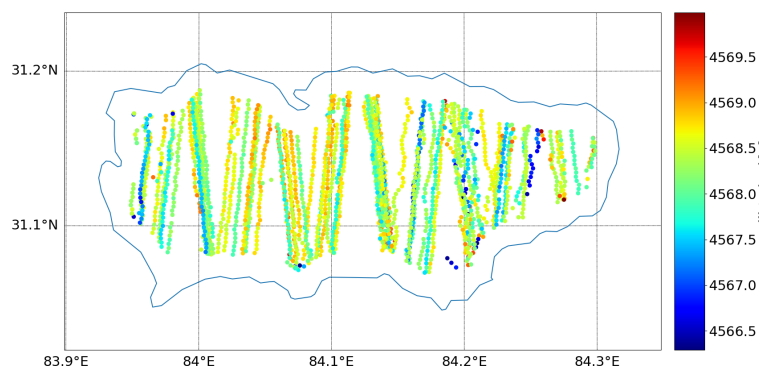
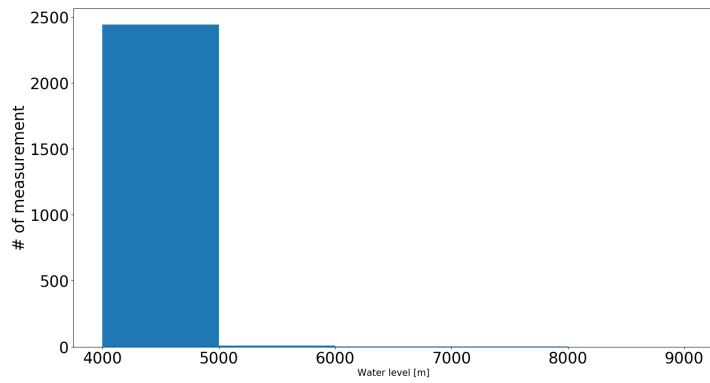
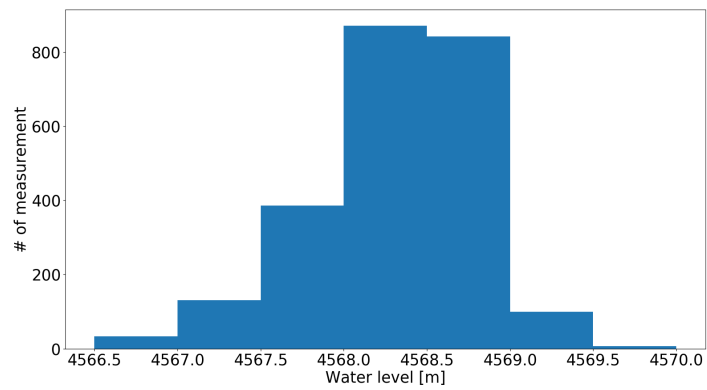


Figure 2.6: Measurements after outlier detection step 2



*Figure 2.7: Histogram of the time series before outlier detection*



*Figure 2.8: Histogram of the time series after outlier detection step 1*

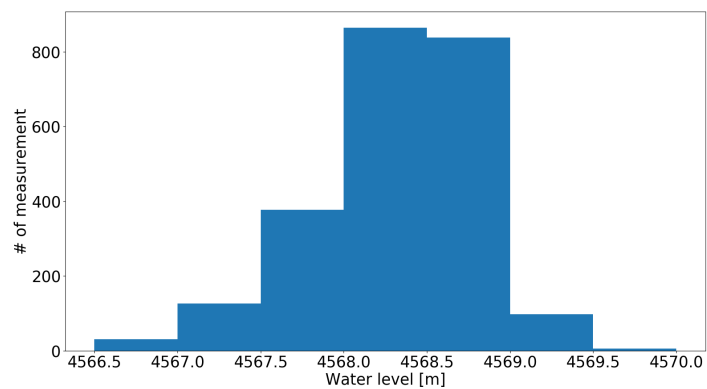


*Figure 2.9: Histogram of the time series after outlier detection step 2*

### 2.3.1 Step 1: global

As can be seen in Fig. 2.4, the ground tracks are relatively obvious. But there are a few red points that indicate extreme values. Because of the red points, the color scale of the water level values are abnormal. Based on the fact that the surface of a quiet lake should have approximately the same water level (orthometric height), the variation of the water level should not be a few kilometres as is shown in the figure. It can also be seen obviously that due to the existence of outliers, the histogram (see Fig. 2.7) seems not in order. Thus, the water level measurements of the whole lake are treated together in outlier detection step 1. According to the normal distribution, the  $4\text{-}\sigma$  criterium is chosen so that the extreme outliers on the whole lake can be eliminated.

After outlier detection step 1, the result seems better. From the total 2453 Taro Co water level measurements, 78 are eliminated. In the colorbar, the water level values look more reasonable. Note that the average water level of Taro Co is really above 4566 metres. The histogram after step 1 is clearly in order as well (see Fig. 2.8).

### 2.3.2 Step 2: track-wise

Still, the color of the points along each ground track does not seem very homogeneous. That is why there is another outlier detection step. In outlier detection step 2, each ground track is treated individually. According to the normal distribution, each track goes through  $3\text{-}\sigma$  criterium which eliminates around 0.3% of the data. Therefore, the outliers of each track are eliminated. In fact, if there is not the global step, a track with many outliers would not be eliminated in this step, because the track would still seem homogeneous. After 29 measurements are eliminated, the tracks seem more homogeneous (see Fig. 2.6). The histogram for it is actually not much different, though (see Fig. 2.9). In fact, only few measurements are eliminated in the track-wise step.

After the two steps of outlier detection, the eliminating ratio of the outliers of this lake is around 4.36%. There are yet some obvious outliers that the data snooping scheme has not detected and eliminated. A possibility to remove them is to use  $2\text{-}\sigma$  instead of  $3\text{-}\sigma$  criterium, which is an even more strict criterium. However, many good measurements would also be eliminated by that, which results in data loss. They tracks look rather broken. So the  $3\text{-}\sigma$  criterium is kept. The outlier detection tool should yet be improved in future work.

## 2.4 Trend computation

The trend of the water level of a lake is a basic question: Does the lake surface rise, or does it sink? And how much? How fast? Since it is strongly related to time, the water level time series should be analyzed according to temporal effects. Although the measurements are the same data (after outlier detection), they are ordered now by the time when they were collected, unrelated to their corresponding geographic locations. Actually, one day pass lasts only a few seconds, thus the measurements on one ground track are taken on the same day. That is also the reason why each ground track should have a rather homogeneous color, which indicates homogeneous water levels.

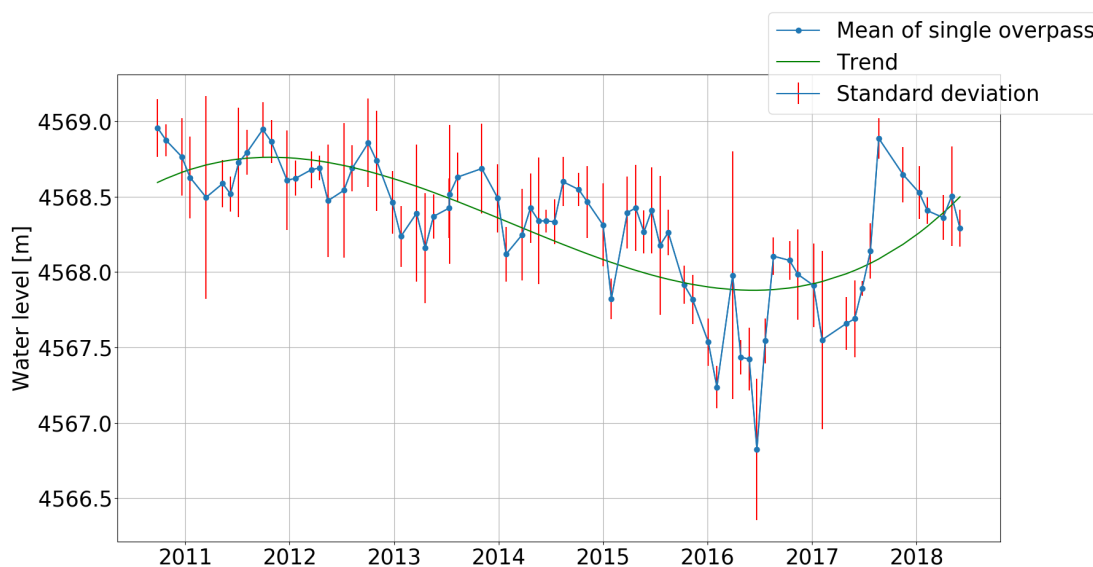


*Figure 2.10: Time series*

Each day is a time point. The first day where there are measurements is September 26, 2010. The next daily mean does not appear one day after that, because CryoSat-2 is not measuring the same lake all the time, it usually takes a month or more to fly over the same lake again. The data collected for this work is available until June in 2018. For each day where measurements are available, the mean of the single pass is calculated. The standard deviation shows how precise the measurements are for each day pass. The mean values are then combined by a line in order to show the tendency better. Based on this combination, a line that approximates it the best represents the trend of water level. As for the lake Taro Co, the trend value is about  $-0.12$  m/yr. It means, this lake is sinking a little bit along with time. An interesting phenomenon is that there is something happening for Taro Co in 2017 that gives the water level a leap. Yet local research cannot be done at this moment. Since this is an independent issue, it is necessary to look at more lakes in Tibet.



## Chapter 3

### Result

As mentioned in chapter 1, Tibet has approximately 400 lakes, over half of them larger than 10 km<sup>2</sup>. The studies of the integrated, global nature of the hydrological cycle are essential to the understanding of natural climate variability. The geographic illustrations of the water level of these lakes indicate the status of each lake. The trend determined helps to predict the future of them. Eight more lakes in Tibet (see Fig. 1.1) are selected and analyzed in the same way as Taro Co. For each lake, a 2D geographic figure with ground tracks as well as a time series figure including trend are generated. Finally, all of the nine lakes contribute to an overview of hydrological pattern of water levels throughout Tibet. This is the main finding of this work.

### 3.1 Selected lakes

#### 3.1.1 Geographic illustrations

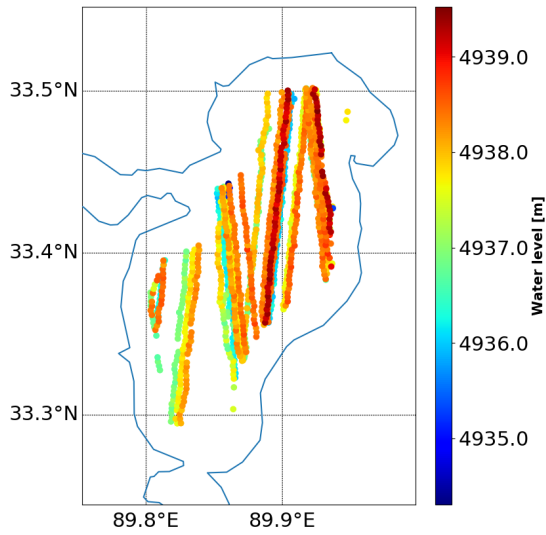


Figure 3.1: Dorsoidong Co

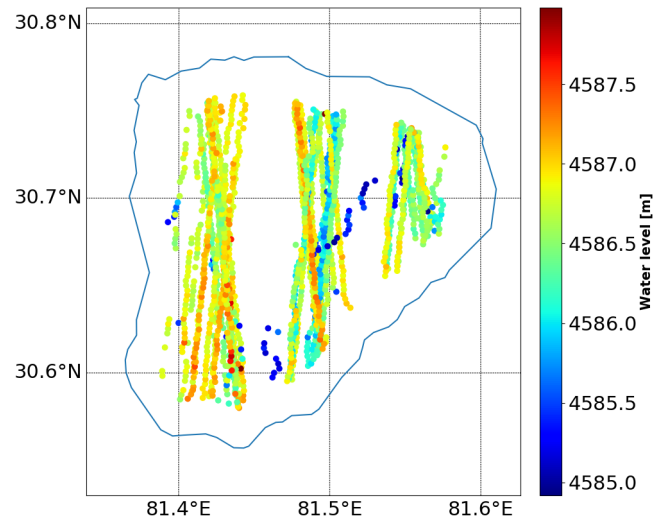


Figure 3.2: Mapam Yumco

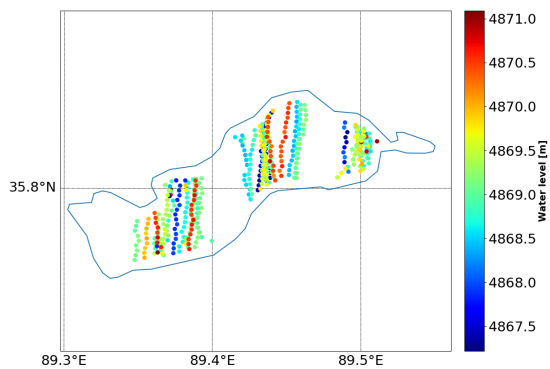


Figure 3.3: Xiangyang Hu

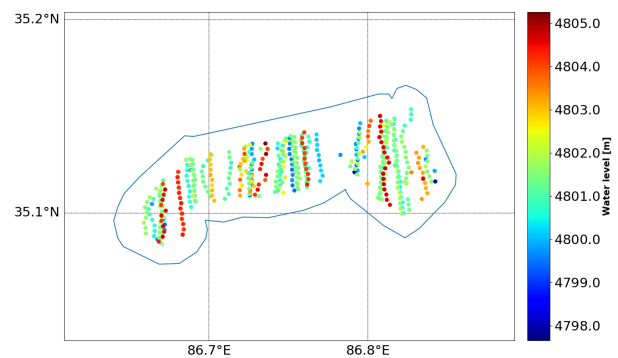


Figure 3.4: Margai Caka

Note that the grid is in  $0.1^\circ \times 0.1^\circ$  which is about 11 km x 11 km.

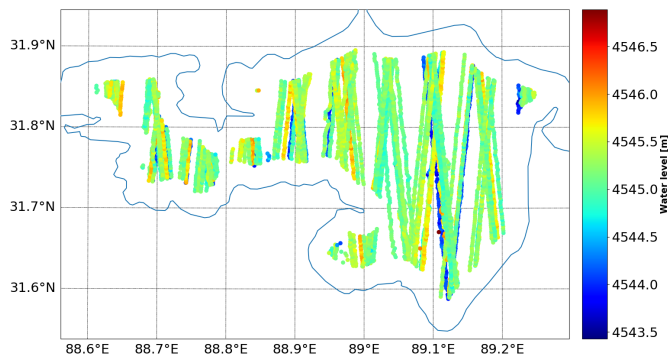


Figure 3.5: Siling Co

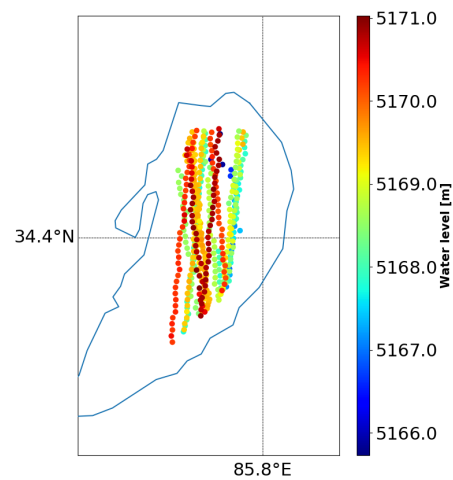


Figure 3.6: Burog Co

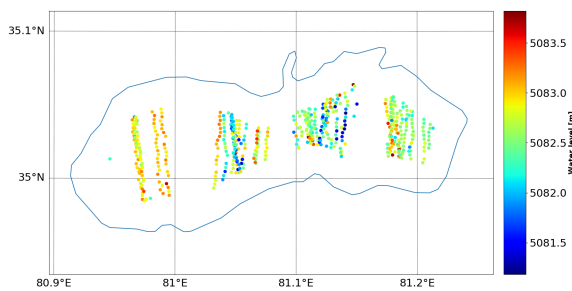


Figure 3.7: Gozha Co

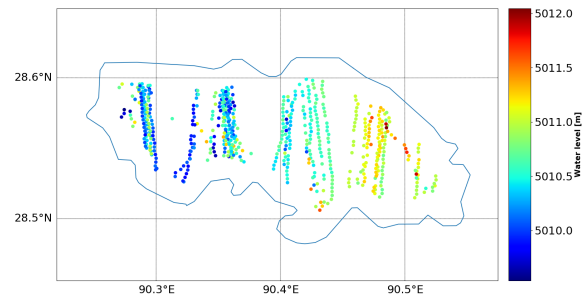


Figure 3.8: Puma Yumco

As can be seen in the eight figures above, the ground tracks are easily discernable. Their homogeneous colors indicate homogeneous values of water levels. Although the big lakes like Mapam Yumco (Fig. 3.2) and Siling Co (Fig. 3.5) still have many outliers at the edge as well as in the middle of the data, their ground tracks are longer than that of small lakes. The large amount of data from the big lakes make the final result, namely the water level, more reliable. As for small lakes like Xiangyang Hu (Fig. 3.3), Margai Caka (Fig. 3.4) and Burog Co (Fig. 3.6), their ground tracks look more homogeneous. For one thing, the total number of measurements on each track is small. Secondly, the changes of the conditions of these small lakes are not as big as that of large lakes. For the case of Gozha Co (Fig. 3.7), it can be detected that there are a few outliers in the very middle of the lake. This may allude to possible small islands in the middle of the lake.

### 3.1.2 Water level time series

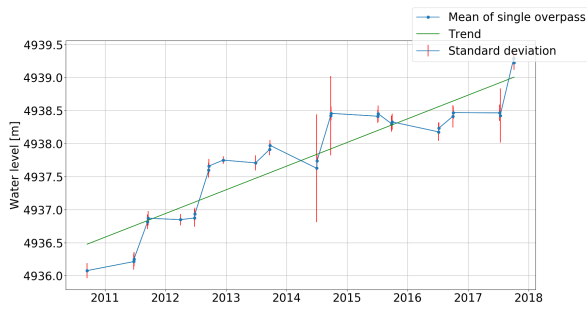


Figure 3.9: Dorsoidong Co

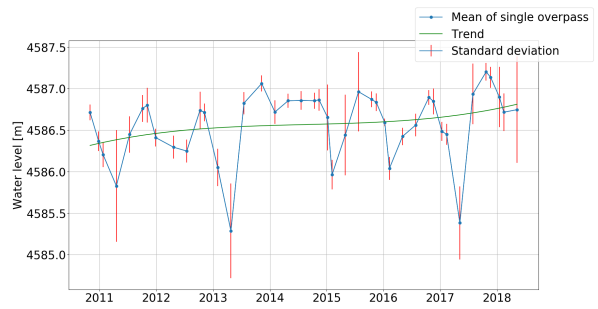


Figure 3.10: Mapam Yumco

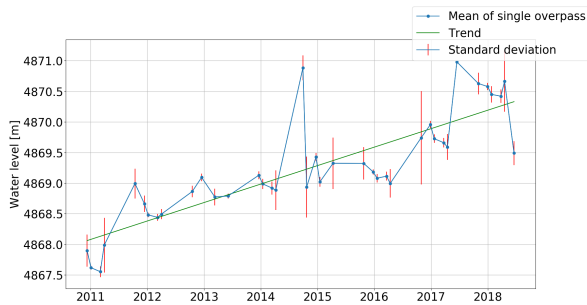


Figure 3.11: Xiangyang Hu

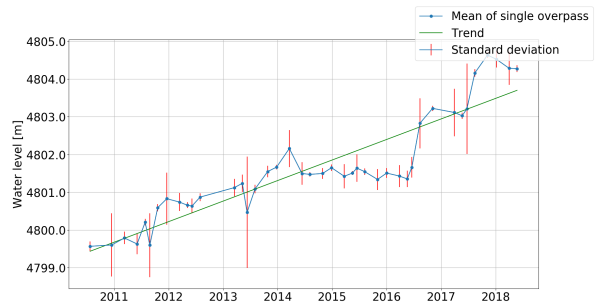
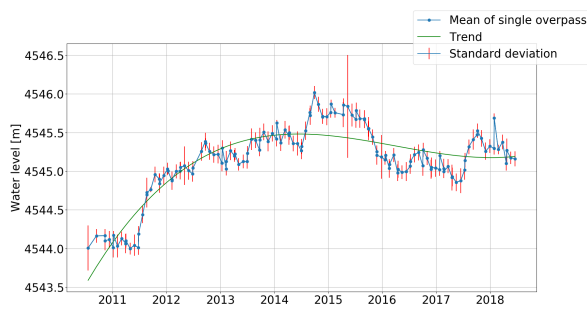
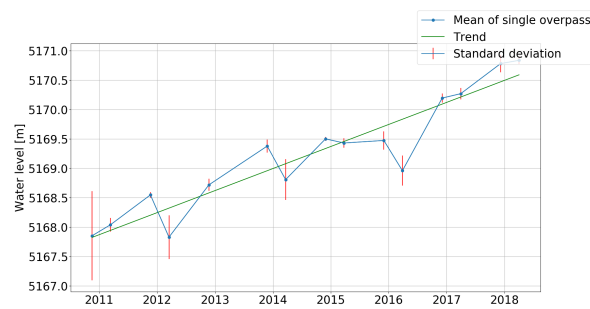


Figure 3.12: Margai Caka



*Figure 3.13: Siling Co*



*Figure 3.14: Burog Co*

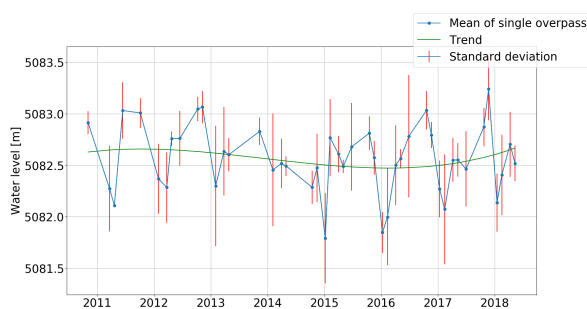


*Figure 3.15: Gozha Co*

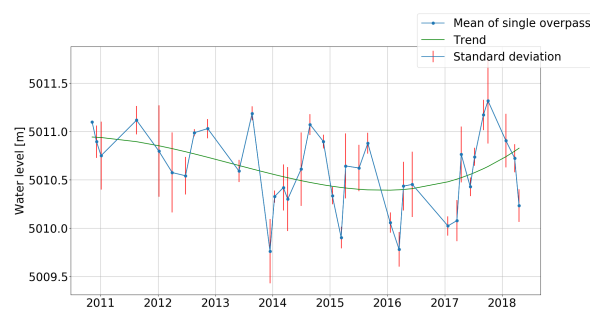


*Figure 3.16: Puma Yumco*

The trend of these selected lake is calculated respectively. While the first six lakes (Dorsoidong Co, Mapam Yumco, Xiangyang Hu, Margai Caka, Siling Co, Burog Co, most of them have a water level under 5000 m) are rising in the last 8 years (2010-2018), the last two (Gozha Co and Puma Yumco) are sinking over this time period. The highest rise is at Margai Cake, which is +0.52 m/yr. It is also because this lake is small. So for the same amount of water input, it rises more. The lake that sinks the most is Taro Co, discussed in the methodology part of this work, whose water level falls with 0.12 m/yr including a leap in 2017. As for the other two lakes that sink, it can be seen that their water levels have an average over 5000 m, so it's more likely that water is going away than coming in. However, Burog Co rises rapidly regardless of its 5158 m water level. This may results from the location of Burog Co since it is in the Northeast of Tibet where the other lakes there are also rising. Geographic effects as well as precipitation may play a role. The numerical values can be found in the Tab. 3.1 in the next section. Besides, it is believed that a seasonal effect is also discernable in most of the lakes. The lakes like Mapam Yumco, Gozha Co and Puma Yumco, for example, are changing only slightly in the last 8 years. But their water levels change a lot during each year in a periodic way. The water level rises in summer when the ice is melting and water flows in. Then it sinks in winter when the lake loses its water. So the end of the year almost matches the beginning. This seanal effect may be analyzed more in future work.

### 3.2 Hydrological pattern

With the help of the trend results, a hydrothologic pattern thourghout the Tibetan area can be illustrated. In the main part of Tibet, a rise of the water levels can be seen, while at the edge, there are lakes which are sinking.

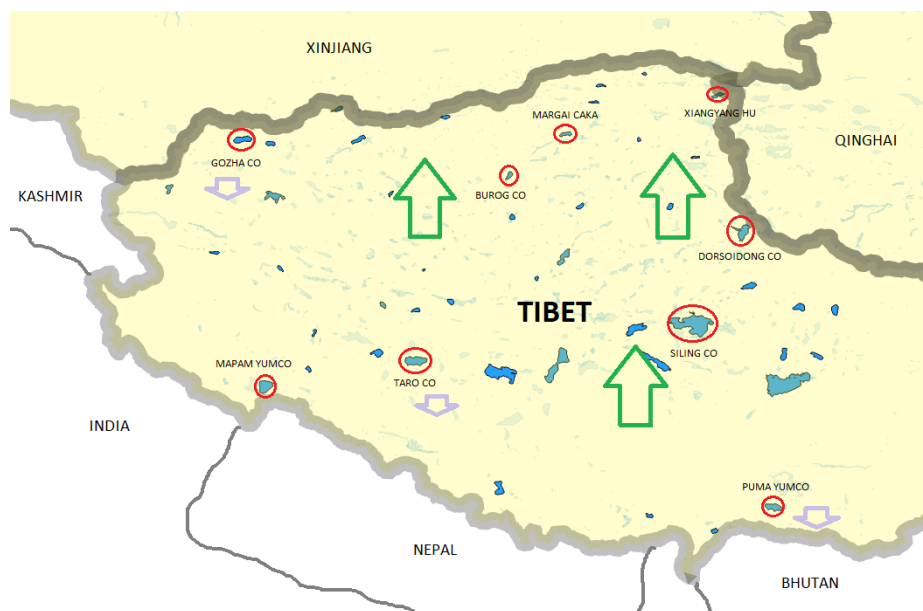


*Figure 3.17: The water level trends of lakes in Tibet*

The numerical information about the trend of these lakes as well as Taro Co can be found in the following table.

Lake name	Size [km <sup>2</sup> ]	Mean water level (2018) [m]	Trend (2010-2018) [m/yr]
Taro Co	486	4566	-0.12
Dorsoidong Co	400	4921	+0.32
Mapam Yumco	412	4556	+0.04
Xiangyang Hu	97	4870	+0.28
Margai Caka	80	4785	+0.52
Siling Co	2391	4530	+0.18
Burog Co	85	5158	+0.35
Gozha Co	253	5080	-0.02
Puma Yumco	280	5030	-0.04

*Table 3.1: Trend results*

The water level monitoring is well improved by satellite altimetry. Since it is known that CryoSat-2 is not the only satellite that does this job. There are many other satellite missions including Jason-2, which may be a comparison especially for water level trends. According to

---

Jason-2 data, while Siling Co rises with 0.26 m/yr and Mapam Yumco with 0.44 m/yr from February 2012 to January 2014, Taro Co sinks with -0.16 m/yr. (Kleinherenbrink et al., 2014 [7]) These trends meet with the trends in the table above. That means, these three lakes are keeping their change in one direction. The other selected lakes in this work are yet not available in the work of Kleinherenbrink. But in that work, it also indicates a positive mass balance in Tibet, which satisfies the Fig. 3.17.





## Chapter 4

### Conclusion

The water level on Tibet, *the third pole*, is analyzed in this work. Nine lakes are selected from Tibet and they represent a hydrological pattern of Tibet properly. The data gap problem is solved by using satellite altimetry mission CryoSat-2. Their measurements are employed and analyzed to determine water level time series in various lakes throughout the Tibetan region. Those time series are subjected to a stepwise outlier detection scheme to identify and eliminate outliers. They are then combined with the local geography to deliver an overview of hydrological pattern throughout Tibet. Furthermore, 30 lakes in Tibet are preliminarily analyzed and the analysis of them should be done in future work.

Global warming is real. The trend of the lakes in Tibet indicates that the water level is rising. The glaciers are retreating rapidly. It is linked to many environmental consequences both locally and globally. As desertification expands, grasslands are shrinking. The regional precipitation has also become irregular. It is affecting nature and civilization in Tibet. Also, the lakes which shrink in the last eight years may disappear if no arrangements are carried out. The monitoring may help people to do something for the control of the rising lakes and the maintenance of the sinking ones.

#### Acknowledgements

To my supervisor, Dr. Hassan Hashemi Farahani and Prof. Dr.-Ing. Nico Sneeuw. Many Thanks! Very special thanks to Dennis Mattes, who has been helping me with the coding in python enormously. Without his help, I would not have been able to design and make the geographic illustrations as well as the hydrological pattern. I appreciate his help sincerely. With a special mention to Elizabeth Woisetschlaeger. It was fantastic to have the opportunity to work majority of my research in her facilities. The method she offered to read the data from ESA plays a big role in my coding part. My forever interested, encouraging and always enthusiastic parents, Yonghong Huang and Dongbing Yan, who were always keen to know what I was doing and how I was proceeding, although it is likely that they have never grasped what it was all about. I am also grateful to the altimetry group: Omid Elmi, Sajedeh Behnia, Tianshu Wang, Bo Wang and Zhuge Xia. And finally, last but by no means least, also to everyone in the impact hub. It was great sharing laboratory with all of you during last four months. Thanks for all your encouragement!



## References

- [1] International conference on climate change. *IOP Conference Series: Earth and Environmental Science*, 200(1):011001, 2018.
- [2] R Floberghagen, M Fehringer, D Lamarre, D Muzi, B Frommknecht, C Steiger, J Piñeiro, and A Da Costa. Mission design, operation and exploitation of the gravity field and steady-state ocean circulation explorer mission. *Journal of Geodesy*, 85(11):749–758, 2011.
- [3] Ch Förste, S Bruinsma, O Abrykosov, JM Lemoine, et al. The latest combined global gravity field model including GOCE data up to degree and order 2190 of GFZ potsdam and GRGS toulouse (EIGEN 6C4). In *5th GOCE user workshop, Paris*, pages 25–28, 2014.
- [4] V Hodge and J Austin. A survey of outlier detection methodologies. *Artificial intelligence review*, 22(2):85–126, 2004.
- [5] SW Hostetler. Hydrological and thermal response of lakes to climate: description and modeling. In *Physics and chemistry of lakes*, pages 63–82. Springer, 1995.
- [6] M Kleinherenbrink, PG Ditmar, and RC Lindenbergh. Retracking cryosat data in the sarin mode and robust lake level extraction. *Remote sensing of environment*, 152:38–50, 2014.
- [7] J Kostelecký, J Klokocník, B Bucha, A Bezdek, and C Förste. Evaluation of the gravity field model EIGEN-6C4 in comparison with EGM2008 by means of various functions of the gravity potential and by gnss/levelling. *Geoinformatics FCE CTU*, 14(1), 2015.
- [8] RD Koster, PR Houser, ET Engman, and WP Kustas. Remote sensing may provide unprecedented hydrological data. *Eos, Transactions American Geophysical Union*, 80(14):156–156, 1999.
- [9] NK Pavlis, SA Holmes, SC Kenyon, and JK Factor. The development and evaluation of the earth gravitational model 2008 (EGM2008). *Journal of geophysical research: solid earth*, 117(B4), 2012.
- [10] R Schneider, PN Godiksen, H Villadsen, H Madsen, and P Bauer-Gottwein. Application of CryoSat-2 altimetry data for river analysis and modelling. *Hydrology and Earth System Sciences*, 21(2):751–764, 2017.
- [11] C Vorosmarty. Nasa post-2002 land surface hydrology mission component for surface water monitoring HYDRA-SAT. In *Report from the NASA Post 2002 LSHP Planning Workshop, Irvine*, volume 53, 2002.